INTERNATIONAL JOURNAL OF SYSTEMATIC AND EVOLUTIONARY MICROBIOLOGY

RESEARCH ARTICLE

Bourland *et al.*, *Int J Syst Evol Microbiol* 2018;68:3052–3065
DOI 10.1099/ijsem.0.002888

MICROBIOLOGY SOCIETY

Morphologic and molecular characterization of *Brachonella pulchra* (Kahl, 1927) comb. nov. (Armophorea, Ciliophora) with comments on cyst structure and formation

William Bourland,[1,*] Johana Rotterová[2] and Ivan Čepička[2]

Abstract

In this article we provide morphologic and morphometric data based on *in vivo* observation, protargol impregnation, scanning electron microscopy and an 18S rRNA gene sequence for another member of the genus *Brachonella*, *Brachonella pulchra* comb. nov. (basionym: *Metopus pulcher* Kahl, 1927). We also provide preliminary data on resting cyst structure and formation in *Brachonella pulchra* and discuss the possible taxonomic usefulness of these structures.

INTRODUCTION

Despite the passage of nearly 250 years since Müller's [1] description of *Metopus es*, efforts to explore the phylogeny of the free-living representatives of Metopida by integrating modern morphologic and molecular methods have only recently begun. Of the nine species currently assigned to *Brachonella* Jankowski, 1964, combined morphologic and molecular data is available only for the type species, *Brachonella contorta* (Levander, 1894; basionym: *Metopus contortus* Levander, 1894) [2].

A recent rekindling of interest in the taxonomy and phylogeny of free-living anaerobic–microaerophilic ciliates has confirmed the non-monophyly of both *Metopus* and *Brachonella*, the two most species-rich genera of the order Metopida Jankowski, 1980 [2]. Since most species of both genera were described before the advent of protargol impregnation and the more modern innovations of electron microscopy and molecular sequencing, there is much work to be done in redescription and molecular characterization of 'old' taxa discovered by early twentieth century workers in addition to identifying new species. Without such efforts a comprehensive and sensible phylogeny of this important group will not be possible. While even many recently described new species lack associated rRNA gene sequences [3–6], others workers have focused mainly on the molecular phylogeny of metopids [7, 8].

Corliss [9] also recognized that the genus *Metopus* would require division into several other genera. This view is further supported by recent molecular phylogenies [8, 10–12]. Jankowski [13] erected the genus *Brachonella* for metopids with a dominant preoral dome, extreme posteriorization of the cytostome and a highly spiralized adoral zone, transferring six species from genus *Metopus*. Many taxa from the genus *Brachonella* Jankowski, 1964 have since been transferred to other genera or synonymized, leaving nine nominal species currently [2, 11, 14, 15]. Combined morphologic and molecular data are available only for the type species, *Brachonella contorta* Jankowski, 1964 [2]. In this report we provide morphologic and morphometric data and an 18S rRNA gene sequence for another member of this genus, *Brachonella pulchra* comb. nov. (basionym: *Metopus pulcher* Kahl, 1927). Although commonly found in the sediments of aquatic habitats, most metopids are likely 'semi-terrestrial' (i.e. encysting in soils and excysting when introduced to aquatic environments or when there is sufficient interstitial water in the soil). Most, if not all, metopids divide in the free-swimming state and, while replication cysts have never been documented in free-living metopids, most species likely do form resting cysts in nature. The diversity of metopid resting cysts has not yet been explored in detail. Little is known about the possible taxonomic significance of resting cysts for metopids in particular or armophorean ciliates in general. Here we also provide preliminary data on resting cyst structure and formation in *Brachonella pulchra*.

METHODS

Collection and culture

The organisms were collected in November 2016, between the towns of Hvězda and Loubí, Czech Republic

Author affiliations: [1]Department of Biological Sciences, Boise State University, Boise, ID 83725-1515, USA; [2]Department of Zoology, Faculty of Science, Charles University, Prague, Czech Republic.
***Correspondence:** William Bourland, willbour@me.com
Keywords: Anaerobic ciliates; extrusome; *Metopus*; phylogeny; Protargol impregnation; 18S rRNA gene.
Abbreviations: MCMC, Markov chain Monte Carlo; PCR, polymerase chain reaction; rRNA, ribosomal RNA; SEM, scanning electron microscopy.
One supplementary movie is available with the online version of this article.

(50°35′54.2″N 14°27′51.2″E), from freshwater sediments with a strong sulfidic odour. Cultures were established as described by Bourland *et al.* [12]. Briefly, non-clonal cultures, including undetermined bacteria, various flagellates and amoebae, were established by inoculating fresh samples into 15 ml Falcon tubes containing 9 ml Sonneborn's *Paramecium* medium [16]. Subcultures were made at intervals of approximately 2 weeks and maintained at room temperature. For studies of cyst formation, cells isolated in 0.22 µm-filtered (Millipore) site water were placed on a slide with a supported coverslip in a moist chamber in an artificial anaerobic environment obtained using AnaeroGen (Oxoid) sachets inserted into a 2.5 l AnaeroJar (Oxoid). Cells were examined at 72 h and 120 h.

Light microscopy

The morphology of living, methyl green–rhodamine B-stained (Waldeck) and protargol-impregnated (Polysciences) cells was examined with a compound microscope. Brightfield and differential interference contrast illumination were used to observe living cells with an Olympus BX53 microscope.

Protargol impregnation was done as previously described [17]. Protargol-impregnated specimens were measured with an ocular micrometer at ×1000 magnification. *In vivo* measurements were made from microphotographs with calibrated Spot imaging software (Diagnostic Instruments). Drawings of live specimens were done free-hand and those of silver-impregnated specimens with the aid of a microscope drawing attachment. Fluorescence microscopy was done with a Zeiss CFL-40 microscope and Zeiss filter set No. 38 (Carl Zeiss). Image stacking was done with Helicon Focus (Helicon Soft Ltd.) to increase depth of focus in some images (Fig. 3A–G). Images were adjusted for brightness, contrast and background removal with Photoshop CS6 (Adobe Systems Inc.).

Scanning electron microscopy

For scanning electron microscopy (SEM), ciliates were selected from cultures under the dissecting microscope, washed in 0.22 µm-filtered Volvic water (French table water), fixed in a solution of glutaraldehyde and osmium tetroxide (2.5 and 1% final concentration, respectively), dehydrated in serial dilutions of ethanol and dried in an EMS 850 critical point dryer (Electron Microscopy Sciences). Dried specimens were mounted on carbon adhesive tabs and sputtered with gold using an Agar sputter coater dryer (Electron Microscopy Sciences). Gold-sputtered specimens were examined in a Hitachi SU3500 scanning electron microscope (Hitachi High Technologies America).

DNA extraction, amplification, cloning and sequencing

Single cells were selected from cultures, washed three times in sterile mineral water, placed individually in PCR tubes containing 50 µl 10 mM Tris–Cl buffer (pH 8.5) and stored at −20 °C prior to extraction. DNA extraction, amplification and sequencing were done as previously described, but using single washed cells [17]. PCR was done in the MJ Mini thermocycler (Bio-Rad) with the following program: 95 °C for 2 min 30 s, 35 identical amplification cycles (95 °C for 30 s, 58 °C for 20 s, 65 °C for 2 min 30 s), 65 °C for 5 min and indefinite hold at 4 °C. PCR products were checked by 1 % (w/v) agarose gel electrophoresis and then purified (ExoSAP-IT, ThermoFisher Scientific). Chromatograms were manually edited using 4-Peaks [18] and assembled into contiguous sequences using CAP3 [19].

Phylogenetic analyses

Three identical single-cell 18S rRNA gene sequences were obtained. We created a data set consisting of the 18S rRNA gene sequences of various Metopida, including the newly determined sequence of *Brachonella pulchra*. The sequences were aligned using MAFFT [20] on the MAFFT 7 server (http://mafft.cbrc.jp/alignment/server/) with the G-INS-i algorithm at default settings. The alignment was manually edited using BioEdit 7.0.9.0 [21]. The final data set of unambiguously aligned characters consisted of 1667 positions (excluding primer sequences) and is available upon request. Modeltest 3.7 [22] was employed to find the model of nucleotide substitution that best fit the data. The general-time-reversible model with invariable sites and gamma distribution (GTR+I+Γ) was chosen under the Akaike information (AI) criterion. Phylogenetic trees were reconstructed by maximum-likelihood (ML) and Bayesian methods. ML analysis was performed in RAxML 8.0.0 [23] under the GTRGAMMAI model. Node support was assessed by ML analysis of 1000 bootstrap data sets. Bayesian analysis was performed using MrBayes 3.2.2. [24] using the GTR+I+Γ+covarion model with four discrete categories. Four Markov chain Monte Carlo (MCMCs) were run for 17 000 000 generations, with a sampling frequency of 500 generations, until the mean standard deviation of split frequencies based on last 75 % was lower than 0.01. The first 25 % of the trees were removed as burn-in.

Terminology

Terminology used in this study is according to [10, 25–28] except as noted. We define the 'preoral dome' as that portion of the cell anterior to the level of the cytostome. The perizonal ciliary stripe is herein referred to as the 'perizonal stripe'. The use of the term 'somatic kineties' excludes perizonal stripe kineties. We define the term 'dome kineties' as kineties the anterior ends of which lie at or above the level of the anterior end of the perizonal stripe and those confined completely to the preoral dome. Classification follows Jankowski [29] and Foissner and Agatha [25] except as noted.

RESULTS AND DISCUSSION

Redescription of *Brachonella pulchra* (Kahl, 1927) comb. nov. based on the HAJENKA population (Czech Republic) (Table 1; Figs 1–6)

Size *in vivo* 90–118×51–71 µm, about 100×62 µm on average (*n*=16), protargol-impregnated specimens 81–106×

Table 1. Morphometric data for the HAJENKA population of *Brachonella pulchra* nov. comb.

Characteristic*	Method†	Mean	M	SD	CV	Min	Max	*n*
Body, length	*In vivo*	100.1	99.0	8.02	8.0	90.0	118.0	16
	P	94.0	94.0	6.55	7.0	81.0	106.0	25
Body, width‡	*In vivo*	62.1	61.0	5.53	8.9	51.0	71.0	16
	P	46.4	46.0	5.74	12.4	33.0	57.0	25
Body, length:width, ratio	*In vivo*	1.6	1.7	0.23	14.2	1.3	2.2	16
	P	2.0	2.0	0.18	8.9	1.8	2.4	25
Anterior cell end to posterior end of adoral zone, distance	*In vivo*	83.6	83.5	6.32	7.6	70.0	96.0	16
	P	77.0	77.0	5.10	6.6	30.0	61.0	25
Distance anterior cell end to posterior end of adoral zone:body length, ratio in %	*In vivo*	83.1	81.5	4.33	5.2	77.0	93.0	16
	P	82.2	82.0	4.49	5.5	76.0	90.0	25
Anterior cell end to posterior margin of macronucleus, distance	*In vivo*	46.3	48.0	6.24	13.5	31.0	54.0	14
	P	48.1	48.0	5.06	10.5	37.0	57.0	25
Distance anterior cell end to posterior margin macronucleus:body length, ratio in %	*In vivo*	46.0	47.0	5.29	11.5	34.0	53.0	14
	P	51.2	52.0	4.67	9.1	39.0	59.0	25
Anterior cell end to posterior end of perizonal stripe, distance	P	70.2	70.0	5.80	8.3	63.0	80.0	15
Anterior cell end to posterior end of perizonal stripe, body length, ratio in %	P	75.1	76.0	5.44	7.2	66.0	86.0	15
Macronucleus, length§	*In vivo*	25.9	26.0	1.46	5.6	23.0	28.0	14
	P	23.1	23.0	2.39	10.3	19.0	29.0	25
Macronucleus, width	*In vivo*	19.8	19.5	2.69	13.6	16.0	26.0	14
	P	15.2	15.0	1.55	10.2	13.0	18.0	25
Micronucleus, length	P	4.2	4.0	0.29	6.9	4.0	5.0	24
Adoral membranelles, number	P	57.1	57.0	2.86	5.0	53.0	63.0	25
Somatic kineties, number	P	34.2	34.0	3.05	8.9	27.0	39.0	25
Preoral dome kineties, number	P	14.3	14.0	0.68	4.8	13.0	16.0	25
Paroral membrane, length§	P	33.1	33.0	2.97	9.0	27.0	40.0	23
Perizonal ciliary stripe rows, number	P	5.0	5.0	0.00	0.0	5.0	5.0	25
Length of mid-ventral adoral membranelle base	P	7.7	8.0	0.80	10.3	7.0	9.0	15

*All distances in µm.

†Measurements and counts (*in vivo*) made from digital images using calibrated software, (P) made from formalin-fixed protargol-impregnated permanent preparations using ocular micrometer.

‡Measured from right margin to left margin of preoral dome.

§Measured as the chord.

CV, coefficient of variation (%); M, median; Max, maximum value; Mean, arithmetic mean; Min, minimum value; *n*, number of cells studied; P, protargol; SD, standard deviation of the arithmetic mean.

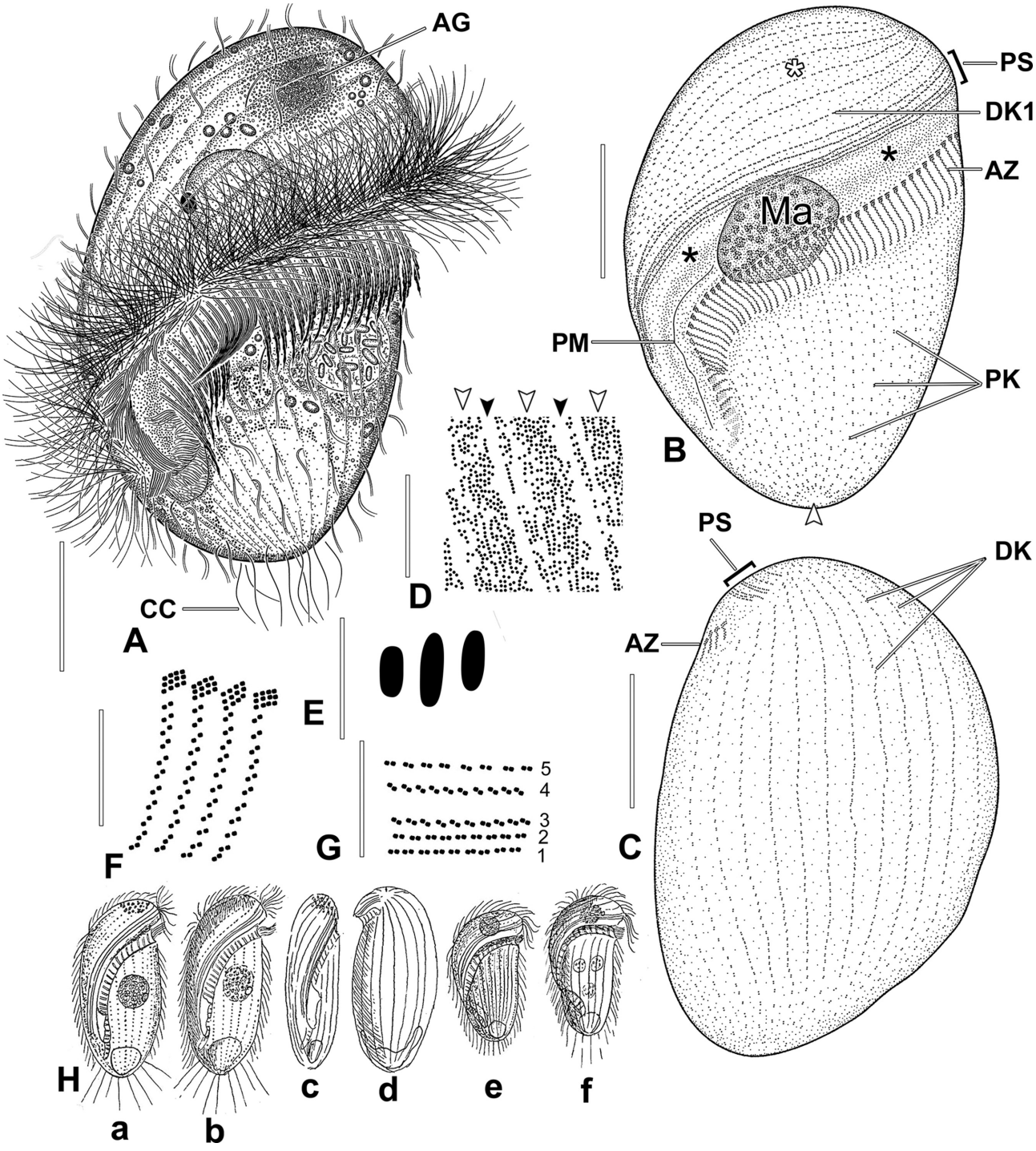

Fig. 1. *Brachonella pulchra* comb. nov. (HAJENKA strain) from life (A, E), after protargol impregnation B, C, F, G), and after staining with methyl green–rhodamine B (D). (A) Typical specimen from life. (B) Ventral view showing small posterior bare area (arrowhead) and undersurface of preoral dome (asterisks). (C) Dorsal view. (D) Loosely arranged granules, probably extrusomes (white arrowheads), between kinetal furrows (black arrowheads). (E) Extrusomes. (F) Morphology of midventral adoral membranelles. (G) Morphology of five-rowed perizonal stripe. (Ha–f) German population of *M. pulcher* from [33] (a–d) and *M. pulcher* var. *tortus* from [35]. AG, anterior granule aggregate; AZ, adoral zone; CC, caudal cilia; DK, preoral dome kineties; DK1, preoral dome kinety1; Ma, macronucleus; PK, postoral kineties; PM, paroral membrane; PS, perizonal stripe; 1–5, perizonal stripe rows 1–5. Bars, 25 µm (A–C), 5 µm (D, F, G), 2.5 µm (E).

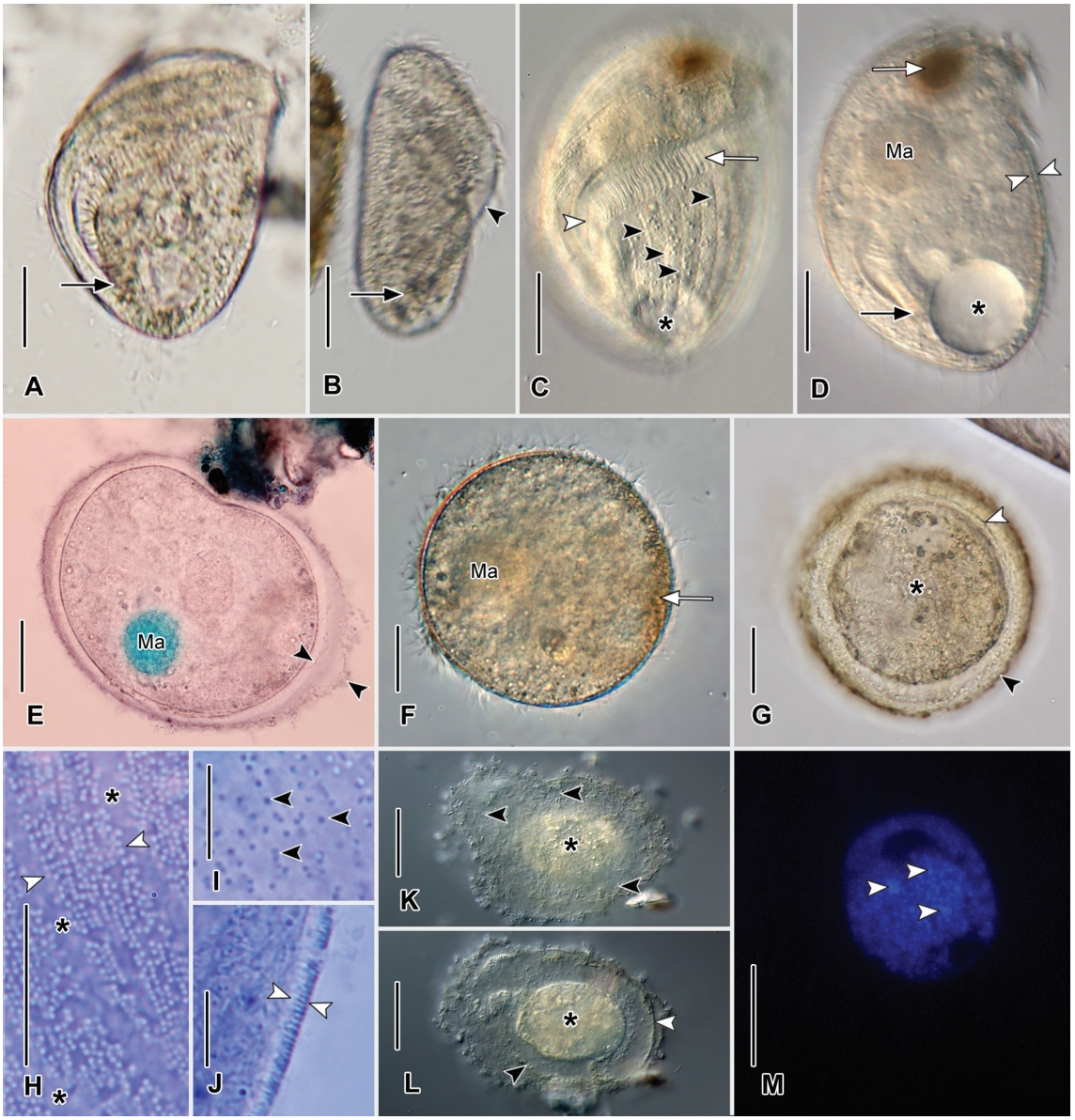

Fig. 2. *Brachonella pulchra* comb. nov. (HAJENKA strain) from life; brightfield illumination (A, B, E–J); differential interference contrast (C, D, K, L); UV fluorescence, (M), after methyl green–pyronin Y staining (E), and after methyl green–rhodamine B staining (H–J). (A) Ventral view showing proximal end of adoral zone (black arrow). (B) Right lateral view showing dorsoventral flattening, the proximal end of adoral zone (black arrow) and the margin of the preoral dome (black arrowhead). (C) Ventral view showing cortical furrows of postoral kineties (black arrowheads), the paroral membrane (white arrowhead), adoral membranelles (white arrow) and contractile vacuole (black asterisk). (D) Optical section showing extrusome layer (between white arrowheads), the anterior granule aggregate (white arrow), proximal end of adoral zone (black arrow) and contractile vacuole in diastole (asterisk). (E) Ejected extrusomes form a mucous sheath (between arrowheads). (F) Early resting cyst showing anterior granule aggregate (white arrow). (G) Five-day-old cyst from anaerobic environment showing decrease in volume of encysted cell (asterisk) and inconspicuous mesocyst layer (white arrowhead) and the thicker ectocyst layer (black arrowhead). (H) Cortical granules, probably extrusomes (between arrowheads), between kineties (asterisks). (I) Cortical granules, probably extrusomes, in the area of the adoral zone (arrowheads). (J) Extrusome layer (between arrowheads). (K, L) Surface view of cyst from open culture vessel (K) showing adherent debris, bacteria and ectocyst (arrowheads) and the enclosed cell (asterisk). Optical section of the same cyst (L) showing ill-defined mesocyst layer (black arrowhead) and more conspicuous ectocyst layer (white arrowhead) surrounding cell (asterisk). (M) Fluorescent endiobionts (arrowheads), probably methanogenic archea. Ma, macronucleus. Bars, 50 µm (K–M), 25 µm (A–E), 10 µm (F, G), 5 µm (H–J).

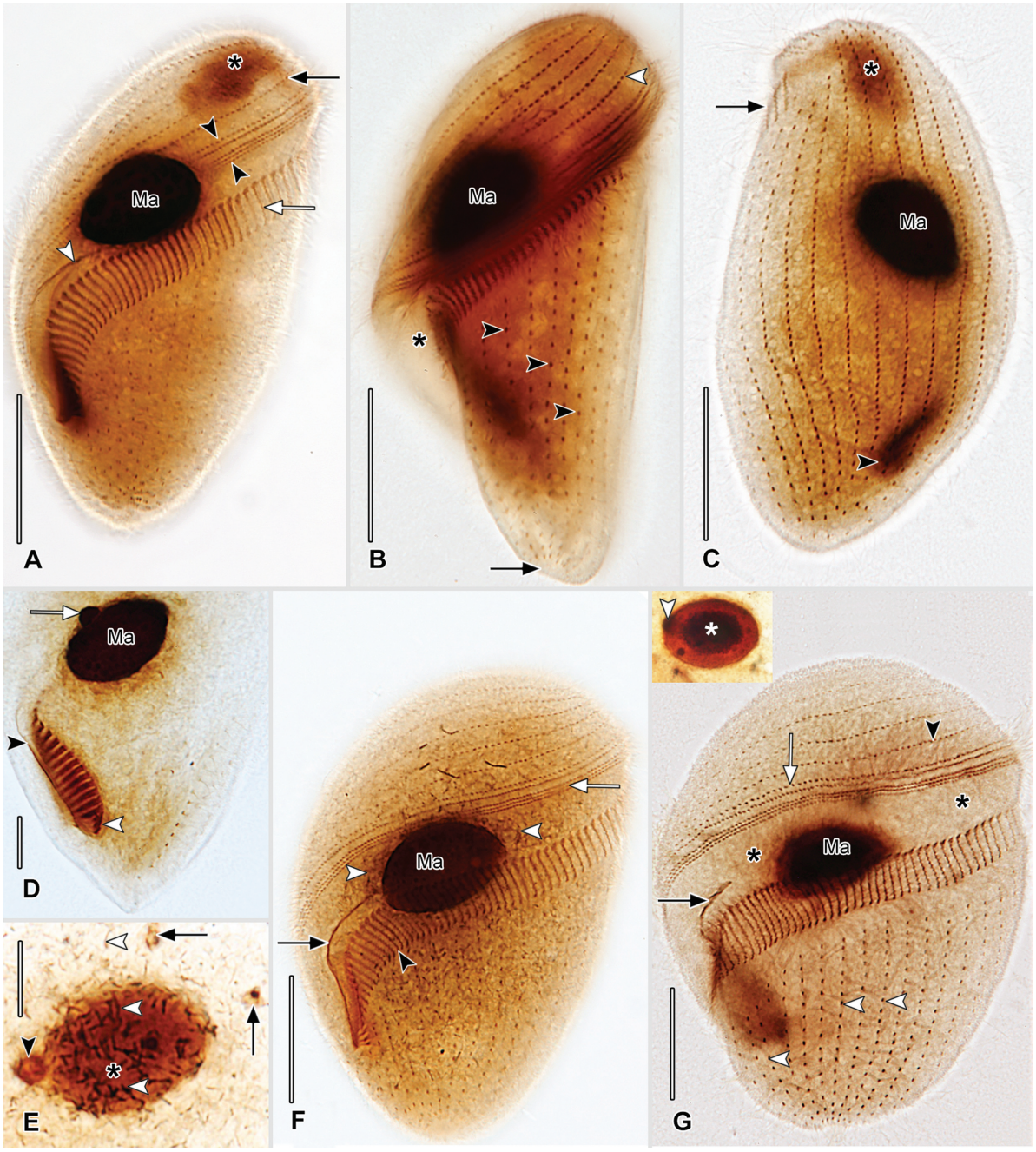

Fig. 3. *Brachonella pulchra* comb. nov. (HAJENKA strain) after protargol impregnation. (A) Ventral view showing anterior granule aggregate (asterisk), perizonal stripe kineties (between black arrowheads), preoral dome kinety 1 (black arrow), the paroral membrane (white arrowhead) and the adoral zone (white arrow). (B) Left lateral view showing dorsoventral flattening of the posterior body part, preoral dome kinety 1 (white arrowhead), postoral kineties (black arrowheads), the undersurface of the preoral dome (asterisk) and the small bare area at the posterior pole (black arrow). (C) Dorsal view showing distal end of the adoral zone (black arrow), level of the cytostome (seen through cell, arrowhead) and the anterior granule aggregate (asterisk). (D) Optical section showing paroral membrane, appearing thickened posteriorly due to associated fibrils (black arrowhead), three small membranelles at the posterior end of the adoral zone (white arrowhead) and the micronucleus (white arrow). (E) Detail view showing argyrophilic rod-shaped cytoplasmic bacteria (white arrowheads) in the region of the macronucleus (asterisk), the micronucleus (black arrowhead) and ingested colourless flagellates (black arrows). (F) Ventral view of intermediate form showing perizonal stripe (white arrow), paroral membrane (black arrow), adoral zone (black arrowhead) and cytoplasmic bacteria surrounding the macronucleus (white arrowheads). (G) Ventral view of 'round' morphotype showing preoral dome kinety 1 (black arrowhead), postoral somatic kineties (white arrowheads), the paroral membrane (black arrow), perizonal stripe (white arrow) and the undersurface of the preoral dome (black asterisks), Inset shows macronucleus of 'round' morphotype with large, ellipsoid central chromatin mass and adjacent micronucleus (white arrowhead). Ma, macronucleus.Bars, 25 µm (A–C, F, G), 10 µm (D, E).

33–57 µm, about 94×46 µm on average (*n*=25). Cell shape broadly ellipsoidal to nearly obovoidal, dorsoventrally flattened about 1.5 : 1 (Figs 1A and 2A–D). Cells shrink asymmetrically with formalin fixation and protargol impregnation distorting the actual shape of the cells (Fig. 1B, C). Preoral dome massive, broadly convex, not twisted, overhangs left cell margin only slightly. Macronucleus ellipsoidal to globular, located in anterior one-half of cell, sometimes in preoral dome (Fig. 2D), chromatin finely granular *in vivo*, scattered small nucleoli in protargol preparations, surrounded by argyrophilic, slender, rod-shaped prokaryotes (Fig. 3E); ellipsoidal micronucleus inconspicuous, adjacent to macronucleus (Figs 1A, B; 2A, D; 3A–E). Contractile vacuole terminal, large (about 25 µm diameter in diastole), with small collecting vesicles, excretory pore terminal, probably temporary, perhaps shared with cytopyge (Figs 1A; 2C, D; 4E). Extrusomes form a peripheral layer, visible *in vivo* (Fig. 2D) and after rhodamine B–pyronin Y (Fig. 2E, G–J), densely spaced in approximately eight interkinetal rows (Fig. 2H, I), ellipsoidal to oblong (i.e. rod-shaped), about 1–1.5 µm long (Fig. 1E), stain bluish-green and often eject with rhodamine B–pyronin Y staining or when distressed, form dense extracellular envelope, do not impregnate with protargol, oblong to cylindrical in SEM when partially ejected (Figs 2E, I–L; 5A–C). Cortex slightly flexible, interkinetal furrows conspicuous (Fig. 2C; Movie S1). Cytoplasm golden-brown, contains numerous 2–3 µm diameter refractive globules, food vacuoles inconspicuous (Fig. 2C). Anterior preoral dome granule aggregate varies from dense, conspicuous to nearly indiscernible (Fig. 2A, C, D, Movie S1, available in the online version of the article). Cytoplasmic prokaryotes not visible *in vivo* but clearly present on UV fluorescence examination, most likely methanogens (Fig. 2M). Swimming pace moderate, steady, frequently lingering over or attached to, detritus (Movie S1).

Somatic kineties non-spiralized (i.e. meridional), ordinarily spaced, comprise 34 rows on average. Ordinary somatic cilia about 7 µm long, perizonal stripe cilia about 15 µm long, several elongated posterior cilia up to 16 µm long. Ciliary rows composed of dikinetids, ordinarily spaced in postoral rows, densely spaced in dorsal rows, both dikinetids in dome region ciliated, usually only posterior basal body ciliated in the postoral body (Fig. 4A, B, E). Somatic kineties end subterminally, leaving small, circular barren area at posterior pole (Figs 1B and 3B). Perizonal stripe invariably composed of densely spaced, completely ciliated dikinetids in five rows; rows 1–3 closely spaced, separated from more widely spaced rows 4 and 5 by a gap, dikinetids of rows 3 and 4 inclined about 45° to kinetal axis; cilia beat in conspicuous metachronal waves (Figs 1A–C, G and 2A–C, F, G; Movie S1).

Adoral zone slightly shorter than perizonal stripe distally, composed of 57 long (7–9 µm at base), very slender membranelles, composed of 3 files of four basal bodies at anterior end and ≥12 inclined rows of two basal bodies posteriorly (Figs 1B, F; 2C and 3A, D, F, G), extends only slightly onto left side anteriorly (Figs 1B, C; 3A–D, F, G). Paroral membrane, long (about 30 % of cell length), stichomonad, (i.e. a single file of ciliated basal bodies), on undersurface of preoral dome, protrudes from buccal cavity (Figs 1B; 2C; 3A, D, F, G; 4A–D; and 5D). Pharyngeal fibres not observed *in vivo* or in protargol-impregnated specimens. Division occurs in the free-swimming state (Fig. 5F).

Notes on 'round' morphotype (Fig. 3G, inset)

In thriving cultures, a morphotype with a broadly triangular to almost circular outline was observed (Fig. 3G), however intermediate forms were also seen (Fig. 3F). The only notable differences from the 'ordinary' morphotype, described above, are (1) a smaller length:width ratio, (2) a slightly narrower adoral zone and (3) an ellipsoidal central macronuclear mass, possibly aggregated nucleoli (Fig. 3G, inset). 'Stout' and 'slender' morphotypes are also characteristic of the more distantly related metopid family, Tropidoatractidae, and may simply reflect body habitus before or after division, the nutritional status or other environmental factors [30].

Cyst formation

Although *Brachonella pulchra* thrived in autoclaved (i.e. deoxygenated) culture medium in closed Falcon tubes, attempts to induce encystment by isolating starved cells under a supported coverglass at atmospheric oxygen concentrations failed. Under these conditions, starved cells became distressed and ejected their extrusomes to form a rather disorganized mucus envelope but then died without completing cyst formation (Fig. 2K, L). When such preparations were placed in an anaerobic environment, cells encysted completely (Figs 2F, G and 5D). This suggests that the process of encystment might be particularly sensitive to oxygen tension. Although we lack a comprehensive understanding of factors inducing encystation in metopids, they probably include those established in other ciliate lineages such as colpodeans and hymenostomes (e.g. starvation or other adverse environmental factors) [14, 31, 32]. Given the anaerobic/microaerophilic lifestyle of metopids, elevated oxygen tension may be an additional adverse environmental factor inducing encystation. However, it is possible that, if the oxygen level rises too high or too rapidly, encystation may be hampered. Extrusomes (mucocysts) are ejected in the first stages of encystment (Fig. 5A–C). The ejected extrusomes then undergo a rather striking transformation to thickened ropy structures forming a dense meshwork of nodular filaments (Fig. 5D, E). Ciliated dikinetids are retained, at least in the early stages of encystation (Fig. 5D). In the light microscope, cysts have a rather ordinary three layered structure including ectocyst, mesocyst and endocyst (not visible as separate from the cell in light microscopy) (Fig. 2G). Viability of cysts was not verified since excystment was not observed.

Occurrence and ecology

Brachonella pulchra was first found by Kahl in sapropelic sediments of a pond in the Hamburg Botanic Garden (site B) during March and April [33]. Kahl also found the slightly smaller, more slender and axially more twisted *M. pulcher*

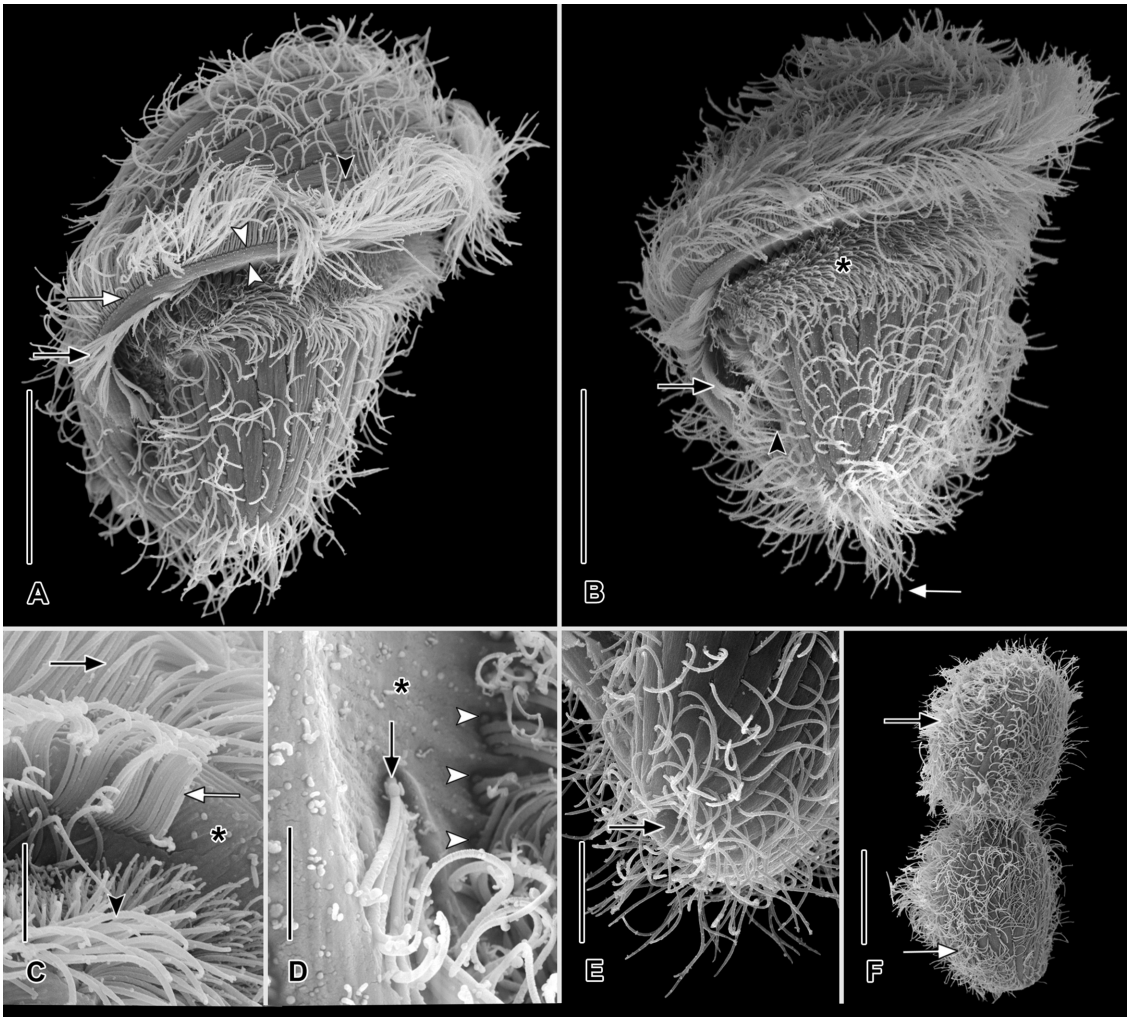

Fig. 4. *Brachonella pulchra* comb. nov. (HAJENKA strain) in the scanning electron microscope. (A) Ventral view showing cilia of the paroral membrane (black arrow), perizonal stripe row 1 (white arrow), brim of the preoral dome (between white arrowheads), and preoral dome kinety 1 (black arrowhead). (B) Ventral view of broader specimen showing paroral membrane (black arrow), cilia of the adoral zone (asterisk), proximal buccal margin (arrowhead) and caudal cilia (white arrow). (C) Detail view of the paroral membrane comprising a single file of cilia (white arrow), cilia of the adoral membranelles (black arrowhead), perizonal stripe cilia (black arrow) and the undersurface of the preoral dome (asterisk). (D) Detail view showing the stichomonad paroral membrane in a cleft on the undersurface of the preoral dome (asterisk) and unciliated basal bodies of the anterior file of the adoral membranelles (arrowheads). (E) Posterior end of the cell showing the excretory pore of the contractile vacuole which may also serve as the cytopyge (arrow). (F) Late divider showing proter (black arrow) and opisthe (white arrow). Bars, 25 µm (A, B, F), 10 µm (E), 5 µm (C), and 2.5 µm (D).

var. *tortus* in a sapropelic moor pond near Hamburg (site S). We found *B. pulchra* in sulfidic freshwater sediments near the north Bohemian village of Loubí, Czech Republic. Food items include bacteria and unidentified colorless heterotrophic flagellates (Fig. 3E). Trophic forms tolerated observation under the cover glass for up to 1 hour but longer exposure to room air resulted in cell death without encystation, indicating limited tolerance to oxygen exposure. The specimens Klein [34] shows as *Metopus pulcher* were sent to him by Kahl and are thus assumed to be from the Hamburg population (probably from the Hamburg Botanic Garden). Jankowski [28] found *M. pulcher*, presumably from freshwater sediments, near Petershoff, on the southern coast of the Gulf of Finland.

Comparison with original description [33] and redescriptions [28, 35] (Figs 1A–G, Ha–f, and 2–4, Table 1)

Kahl originally found two morphotypes of *Metopus pulcher*, a larger (about 80 µm in length), less 'twisted' form from the Hamburg Botanic Garden (site B) and a smaller (about 65–70 µm in length) more 'twisted' form from the moor shooting range pond (site S) [33]. The latter was considered as a variety of the former, *Metopus pulcher* var. *tortus*, but Kahl

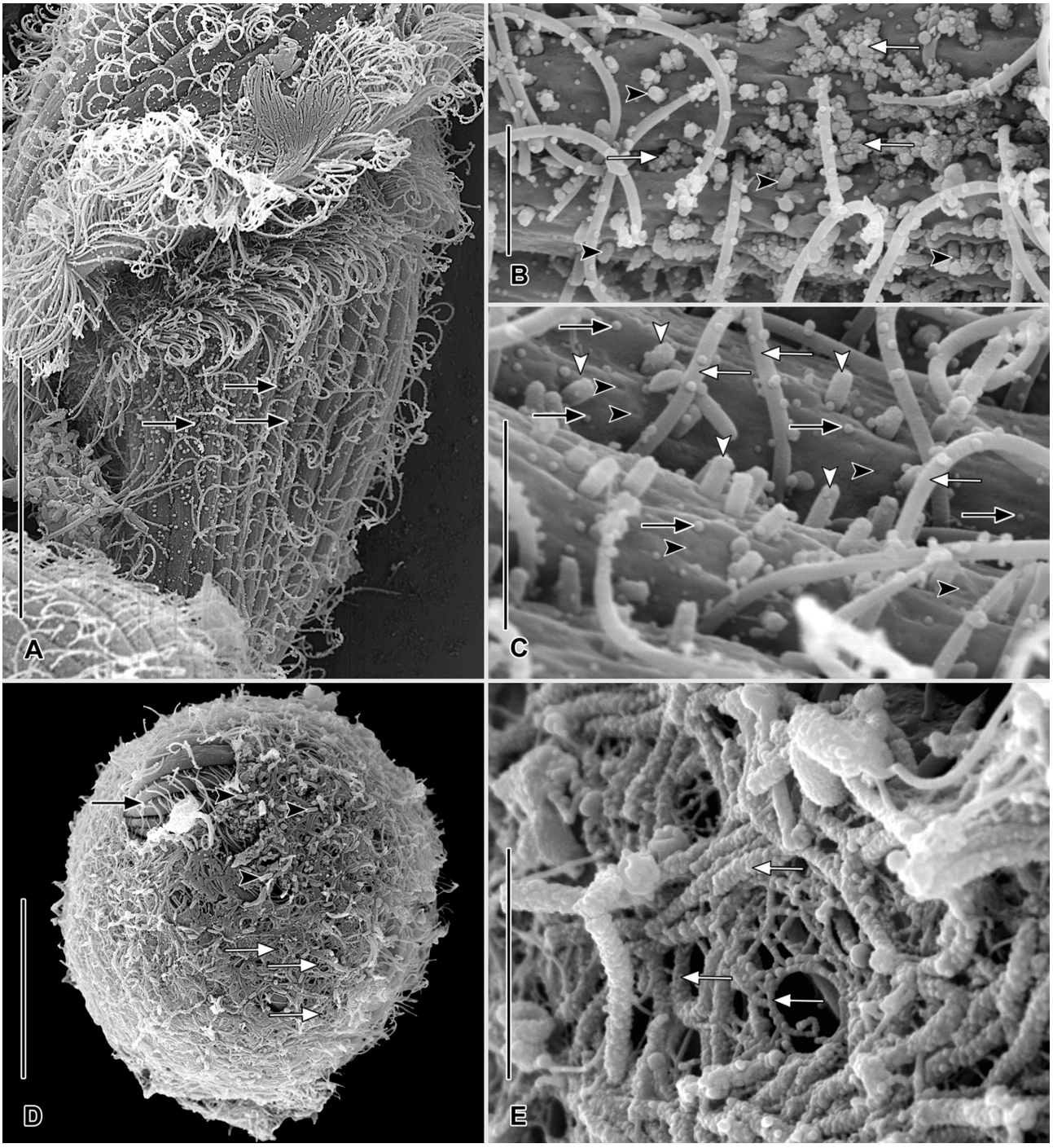

Fig. 5. *Brachonella pulchra* comb. nov. (Hajenka strain) in the scanning electron microscope. (A) Ventral surface of cell with ejecting interkinetal extrusomes (black arrows). (B) Detail view showing ejecting extrusomes (black arrowheads) and coalescing globular material of uncertain origin (arrows). (C) Detail view showing ejecting extrusomes (white arrowheads), somatic cilia (white arrows), and tiny globules (black arrows) emerging from inconspicuous cortical pits (black arrowheads). (D) Cyst (probably early stage) showing the still ciliated encysting cell seen through a tear in the cyst wall (black arrow), the fibrillar meshwork of the cyst wall (white arrows) with sparse adherent bacteria (black arrowheads). (E) Detail of the developing cyst wall (same specimen as [D]) showing a meshwork of fibrils coated with globular material (white arrows). Scale bars: 25 µm (A, D), 2.5 µm (B, C, E).

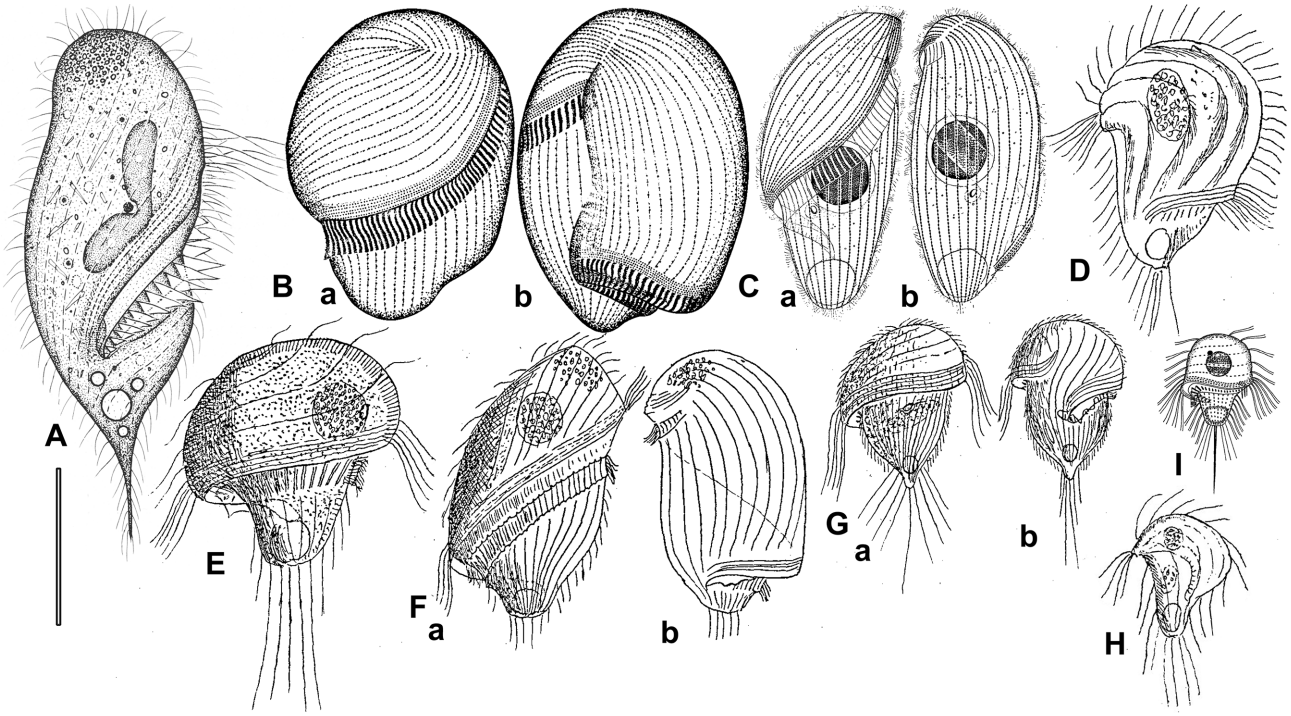

Fig. 6. (A) *Brachonella lemani* (modified from [36]). (B) *Brachonella mitriformis*. Dorsal (a) and ventral (b) views (modified from [37]). (C) *Brachonella elongata*. Ventral (a) and dorsal (b) views (modified from [28]). (D) *Brachonella pyriformis*. Ventral view. (E) *Brachonella intercedens*. Dorsal view. (F) *Brachonella contorta*. Dorsal (a) and ventral (b) views (G) *Brachonella cydonia*. Dorsal (a) and right ventrolateral (b) views. (H) *Brachonella fastigata*. Dorsal (a) and ventral (b) views (D–H modified from [33]). (I) *Brachonella caenomorphides*. Dorsal view, according to terminology used herein (modified from [38]). Bar, 50 µm. Sizes for (D, E, F, G, H) approximate since range, but not exact size, given for original figures).

subsequently stated that *M. pulcher* var. *tortus* could possibly be a separate species. In the Czech population, we did not observe forms closely matching Kahl's *M. pulcher* var. *tortus*. Both forms were described as quite variable, including 'transitional forms' (possibly a result of environmental factors) and redescription of both morphotypes gave a larger upper limit for the length of both morphotypes (about 110 µm) [35]. The Czech population closely matches the Hamburg Botanic Garden population in the following features mentioned by Kahl [33, 35]: size (length, 90–118 µm, average 100 µm (n=16) versus 80–110 µm, macronuclear shape and position (globular, sometimes in preoral dome versus spherical, sometimes in preoral dome), colour (golden-brown versus yellowish to brownish), extrusomes (rod-shaped in about eight interkinetal rows in both), interkinetal distance (4–6 µm versus approximately 5 µm), position of cytostome or 'pharyngeal funnel' (strongly posteriorized in both, and elongated posterior cilia (present in both) [33, 35]. Some differences between the Czech and German populations are noted, including the earlier description of a violet to 'rosy' colour of the cytoplasm (depending on type of illumination) [33]. This discrepancy may reflect greater availability and consumption of purple sulfur bacteria in the German population. The German population was also somewhat more slender [length:width ratio of Czech population 1.3–2.2 *in vivo*, average 1.6 (n=16) versus a single value of 2.3], possibly reflecting nutritional status.

Generic classification and establishment of the new combination

Jankowski [13] established the genus *Brachonella* for Metopidae with the following diagnostic characters: 'anterior body part greatly enlarged, posterior one is reduced in length; peristome long, narrow, spiraling (S-like); the cytostome is shifted by the extremely developed buccal cavity, to the posterior extremity, dorsally; the left-sided body torsion is perfectly developed in all species'. The meaning of the last character ('perfectly developed' left-side torsion), is unclear. Jankowski redescribed *Metopus pulcher* from a mercuric chloride-fixed Russian population. It is puzzling that he chose not to include it in his new genus, *Brachonella*, since it had all of the generic diagnostic features. This is even more surprising since Kahl had already suggested a close relationship between *Metopus pulcher* and *Brachonella contorta* [33].

Jankowski's written description of the 'anterior body part' (the 'preoral dome' herein) comprising <50 % of the body length (anterior body part about 44 µm; cell length about 94 µm) conflicts with his drawings that show it as about 84 % of the body length. The latter figure is consistent with Kahl's description

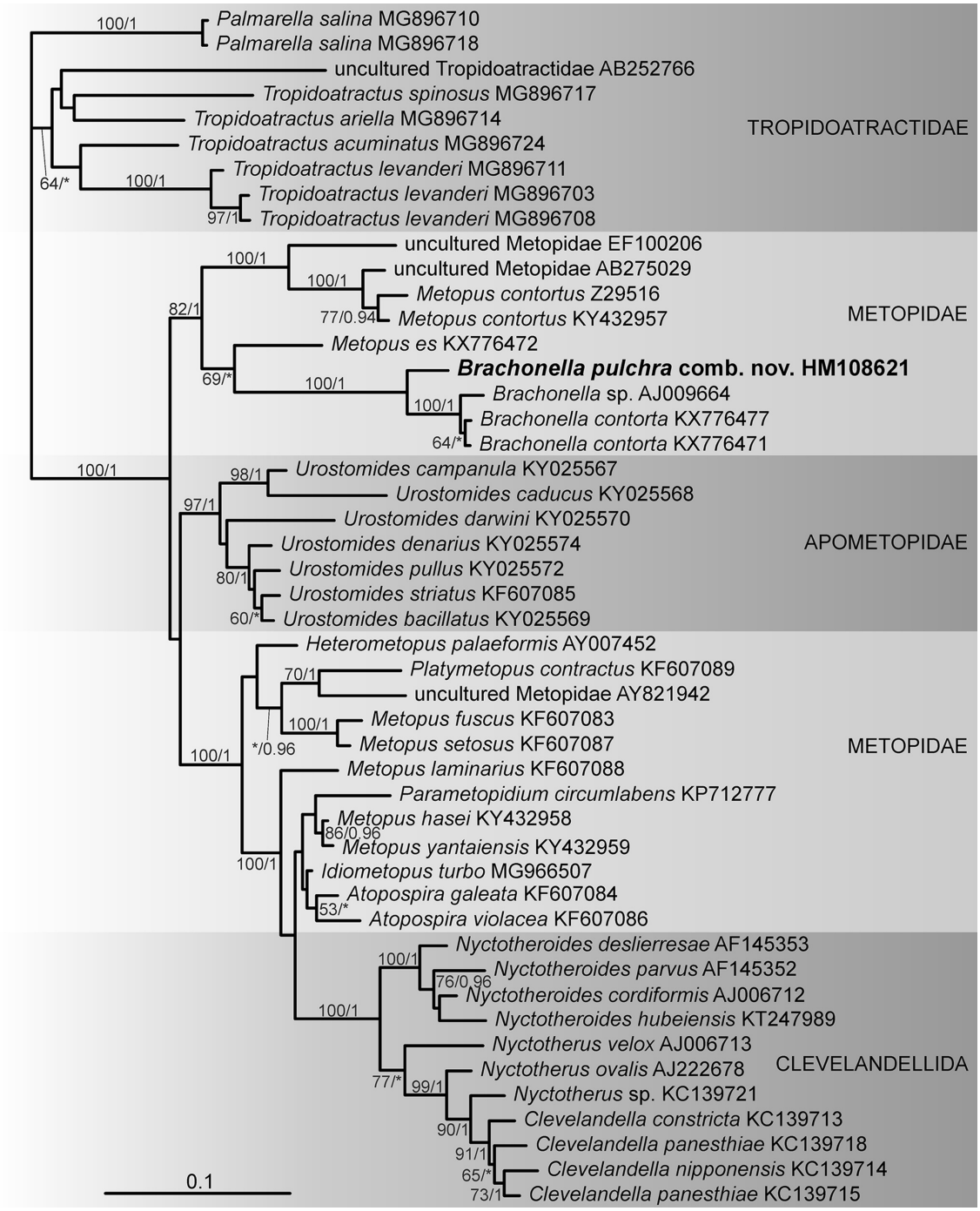

Fig. 7. Unrooted phylogenetic tree based on the 18S rRNA gene sequences showing the phylogenetic position of *Brachonella pulchra* comb. nov. The tree was reconstructed by the maximum-likelihood method in RAxML. The values at branches represent statistical support in bootstrap values (RAxML)/posterior probabilities (MrBayes). Support values below 50/0.90 are not shown or are represented by an asterisk (*). New sequence in bold. GenBank accession numbers follow taxon names. Bar, 10 changes per 100 positions.

and the Czech population described in this report. As was often the case, Jankowski's drawings of interkinetal distances and interkinetidal distances are probably unreliable [12]. The paroral membrane (undulating membrane) is described as 'large and distinct' but is almost indiscernible in the drawings ([28], Fig. 14a–d). We consider the Russian population to be conspecific with Hamburg Botanic Garden population and with the Czech (HAJENKA) population. Because the Czech

population has all of the diagnostic generic features mentioned (preoral dome about 84 % of cell length, and cytostome shifted near the posterior end of the cell), we transfer *M. pulcher* to the genus *Brachonella.*

Remarks

We reject the synonymy of *Metopus pulcher* and *Urostomides striatus* (formerly *Metopus striatus*), as proposed by Esteban *et al.* [14], since the genus *Urostomides* is characterized by a four-rowed, as opposed to the five-rowed, perizonal stripe of *B. pulchra* [12].

Comparison with related species (Fig. 6A–H)

Levander depicted a ciliate ([2] Plate 1, Fig. 2) he identified as *Metopus sigmoides* (a junior synonym of *M. es*), but considered by Kahl to be a different species very similar to *Metopus pulcher* [3]. *Brachonella pulchra* superficially resembles several medium-sized metopids, including *Metopus barbatus* Kahl, 1927, *M. ovalis* [33, *M. contortus* Levander, 1894, and *M. inversus* (basionym: *Brachonella inversa* Jankowski, 1964). Although also differing in features such as macronuclear shape, number of ciliary rows, habitat and so on, the most obvious difference from the latter four taxa is the marked posteriorization of the cytostome in *B. pulchra* (in the posterior 20 % of the cell in *B. pulchra* versus approximately equatorial in the other metopids listed).

Brachonella pulchra should not be confused with the type species of the genus, *B. contorta* due to: the shape of the preoral dome (broadly rounded versus conical), the anterior ciliary suture (absent versus present), number of ciliary rows (34 on average versus usually >50), the degree of adoral zone spiralization (minimal versus about 360°) and the shape of the posterior end (broadly rounded versus truncate obconical) [2]. The remainder of the species currently included in *Brachonella* have not been well characterized by modern morphologic or molecular methods so strict comparisons are difficult, but even with this limited information *Brachonella pulchra* can be distinguished from these congeners (Fig. 6A–H). It can be distinguished from *B. cydonia* [33] by the overall body shape (ellipsoidal versus broadly fusiform) and the shape of the posterior end and distribution of caudal cilia (broadly rounded, elongated caudal cilia dispersed versus narrowly tapered, caudal cilia as discrete tuft) [28, 33]. *Brachonella pulchra* differs from *B. elongata* Jankowski, 1964 in its ciliature (preoral dome suture absent versus present) and the spiralization of the adoral zone (minimal versus >270°) [13, 28]. *Brachonella pulchra* is distinguished from *B. fastigata* [33] by body shape (broadly ellipsoidal versus pyriform) and size (100 µm on average versus about 50 µm) [33]. *Brachonella pulchra* clearly differs from *B. intercedens* [33] in body shape (broadly ellipsoidal versus pyriform) and size (100 µm on average versus about 40 µm) [33]. *Brachonella pulchra* is easily distinguished from *B. lemani* [36] by body shape (posterior end broadly rounded versus posterior end forming long pointed tail), shape of the macronucleus (broadly ellipsoidal versus elongated sausage-shape with central invagination) [36]. *Brachonella pulchra* differs from *B. mitriformis* Alekperov, 1984 in body shape (broadly ellipsoidal versus broadly fusiform anteriorly, short, bluntly tapered posterior end), ciliature (anterior suture absent versus present) and spiralization of the adoral zone (minimal versus about 360°) [37]. *Brachonella pulchra* is easily distinguished from *B. caenomorphides* Foissner, 1980 on the basis of size (medium versus small), shape (broadly ellipsoidal versus campanulate), the posterior cilia (not clumped versus clumped) and number of perizonal stripe kineties (five versus less than five) [38]. The latter feature may indicate a different generic position for this species (possibly *Urostomides*), but we prefer to leave it in the genus *Brachonella* pending a detailed redescription.

Phylogenetic position (Fig. 7)

Phylogenetic analyses based on the 18S rRNA gene sequence fully support the close relationship of *B. pulchra* to the type species of *Brachonella*, *B. contorta*.

Possible taxonomic significance of armophorean resting cysts

Resting cyst morphology is of major taxonomic importance, at least at species level, in groups such as the classes Colpodea and Oligotrichea, and the non-euplotid hypotrichs [39, 40]. The scant data available on metopid resting cysts indicate at least two morphologic types: (1) smooth, transparent, flask-shaped cysts with an apical excystment site ('escape' apparatus or 'operculum') in *Heterometopus palaeformis* (basionym *M. palaeformis* [33] ([14], Fig. 60) and some clevelandellids [41], (2) rough, spherical cysts with a coarse fibrillar exocyst in the genetically distinct *B. pulchra* (current report, Figs 2E–G, K, L and 5A–E). The possible taxonomic and phylogenetic importance of resting cysts in this group will become clear only when detailed data are available for resting cyst morphology and formation in the other main clades of Armophorea.

TAXONOMIC SUMMARY

Ciliophora: Intramacronucleata: Armophorea: Metopida: Metopidae Kahl, 1927 Genus *Brachonella* Jankowski, 1964.

Improved diagnosis: Medium-sized Metopidae, appearance bulky; usually with cortical granules; disproportionately large preoral dome overhanging elongated adoral zone of membranelles, adoral membranelles composed of long files of basal bodies, in deep groove, degree of adoral zone spiralization quite variable, pitch of adoral zone spiral variable; paroral membrane a single file of basal bodies; cytostome displaced posteriorly.

Remarks: the diagnosis is improved here to reflect the rather high variability in degree of adoral zone pitch and spiralization and to include to stichomonad structure of the paroral membrane. The key diagnostic features of the genus *Brachonella* are the extreme posteriorization of the cytostome together with a five-rowed perizonal stripe.

Brachonella pulchra (Kahl, 1927) comb. nov

Metopus pulcher Kahl, 1927.

Etymology: pul'chra. L. fem. adj. pulchra- beautiful, handsome.

Diagnosis based on the original description (Kahl, 1927) and the HAJENKA (Czech Republic) population: Size about 100×60 µm *in vivo*, about 95×45 µm after protargol impregnation. Cell shape broadly ellipsoidal to nearly obovoidal, dorsoventrally flattened about 1.5 : 1. About 34 non-spiralized somatic kineties on average, of which about 14 extend onto preoral dome. Adoral zone spirals only slightly onto dorsal side anteriorly, composed of about 57 adoral membranelles. Freshwater habitat.

Voucher material: two slides with protargol-impregnated voucher specimens of the HAJENKA population are deposited in the collection of the National Museum in Prague, Czech Republic, inventory numbers P6E 4830 and P6E 4831 Relevant specimens are marked with black ink circles.

Funding information
This work was supported, in part, by funds from GAUK (project 389915) and research grant SVV 260434/2018.

Acknowledgements
The authors would like to thank Kateřinka Poláková, Dept. of Zoology, Charles University, Prague, Czech Republic for kindly obtaining the sample from which *Brachonella pulchra* was recovered.

Conflicts of interest
The authors declare that there are no conflicts of interest.

References

1. Müller OF. *Zoologiae Danicae Prodromu*. Havniae; 1776. p. 282.
2. Bourland W, Rotterova J, Čepička I. Redescription and molecular phylogeny of the type species for two main metopid genera, *Metopus es* (Müller, 1776) Lauterborn, 1916 and *Brachonella contorta* (Levander, 1894) Jankowski, 1964 (Metopida, Ciliophora), based on broad geographic sampling. *Eur J Protistol* 2017;59:133–154.
3. Foissner W, Agatha S, Berger H. Soil ciliates (Protozoa, Ciliophora) from Namibia (Southwest Africa), with emphasis on two contrasting environments, the Etosha Region and the Namib Desert. Part I: text and line drawings. *Denisia* 2002;5:1–1063.
4. Vďačný P, Foissner W. A huge diversity of metopids (Ciliophora, Armophorea) in soil from the Murray River floodplain, Australia. II. Morphology and morphogenesis of *Lepidometopus platycephalus* nov. gen., nov. spec. *Acta Protozool* 2017;56:39–57.
5. Foissner W. *Heterometopus meisterfeldi* nov. gen., nov. spec. (Protozoa, Ciliophora), a new metopid from Australia. *Eur J Protistol* 2016;55:118–127.
6. Vďačný P, Foissner W. A huge diversity of metopids (Ciliophora, Armophorea) in soil from the Murray River floodplain, Australia. I. Description of five new species and redescription of *Metopus setosus* Kahl, 1927. *Eur J Protistol* 2017;58:35–76.
7. Hirt RP, Dyal PL, Wilkinson M, Finlay BJ, Roberts DM *et al.* Phylogenetic relationships among karyorelictids and heterotrichs inferred from small subunit rRNA sequences: resolution at the base of the ciliate tree. *Mol Phylogenet Evol* 1995;4:77–87.
8. da Silva Paiva T, do Nascimento Borges B, da Silva-Neto ID. Phylogenetic study of Class Armophorea (Alveolata, Ciliophora) based on 18S-rDNA data. *Genet Mol Biol* 2013;36:571–585.
9. Corliss JO. *The Ciliated Protozoa: Characterization, Classification, and Guide to the Literature*. Oxford, London, New York, Paris: Pergamon Press; 1961.
10. Bourland WA, Wendell L, Hampikian G. Morphologic and molecular description of *Metopus fuscus* Kahl from North America and new rDNA sequences from seven metopids (Armophorea, Metopidae). *Eur J Protistol* 2014;50:213–230.
11. Bourland WA, Wendell L. Redescription of *Atopospira galeata* (Kahl, 1927) nov. comb. and *A. violacea* (Kahl, 1926) nov. comb. with redefinition of *Atopospira* Jankowski, 1964 nov. stat. and *Brachonella* Jankowski, 1964 (Ciliophora, Armophorida). *Eur J Protistol* 2014;50:356–372.
12. Bourland W, Rotterová J, Čepička I. Morphologic and molecular characterization of seven species of the remarkably diverse and widely distributed metopid genus *Urostomides* Jankowski, 1964 (Armophorea, Ciliophora). *Eur J Protistol* 2017;61:194–232.
13. Jankowski AW. Morphology and evolution of Ciliophora I. The new system of sapropelobiotic Heterotrichida. *Zool Zhurnal* 1964;43: 503–517.
14. Esteban G, Fenchel T, Finlay B. Diversity of free-living morphospecies in the ciliate genus *Metopus*. *Archiv für Protistenkunde* 1995;146:137–164.
15. Foissner W. Taxonomische Studien über die Ciliaten des Grossglocknergebietes IX. Ordnungen Heterotrichida Und Hypotrichida. *Ber Nat-Med Ver Salzbg* 1980;5:71–117.
16. Sonneborn TM. Methods in *Paramecium* research. *Methods Cell Physiol* 1970;4:241–339.
17. Bourland WA, Hampikian G, Vďačný P. Morphology and phylogeny of a new woodruffiid ciliate, *Etoschophrya inornata* sp. n. (Ciliophora, Colpodea, Platyophryida), with an account on evolution of platyophryids. *Zool Scr* 2012;41:400–416.
18. Griekspoor A, Groothuis T. 2006. 4Peaks. Available from http://mekentosj.com.
19. Huang X, Madan A. CAP3: A DNA sequence assembly program. *Genome Res* 1999;9:868–877.
20. Katoh K, Misawa K, Kuma K, Miyata T. MAFFT: a novel method for rapid multiple sequence alignment based on fast Fourier transform. *Nucleic Acids Res* 2002;30:3059–3066.
21. Hall TA. BioEdit: a user-friendly biological sequence alignment editor and analysis program for Windows 95/98/NT. *Nucleic Acids Symp Ser* 1999;41:95–98.
22. Posada D, Crandall KA. MODELTEST: testing the model of DNA substitution. *Bioinformatics* 1998;14:817–818.
23. Stamatakis A. RAxML version 8: a tool for phylogenetic analysis and post-analysis of large phylogenies. *Bioinformatics* 2014;30: 1312–1313.
24. Ronquist F, Teslenko M, van der Mark P, Ayres DL, Darling A *et al.* MrBayes 3.2: efficient Bayesian phylogenetic inference and model choice across a large model space. *Syst Biol* 2012;61:539–542.
25. Foissner W, Agatha S. Morphology and morphogenesis of *Metopus hasei* Sondheim, 1929 and *M. inversus* (Jankowski, 1964) nov. comb. (Ciliophora, Metopida). *J Eukaryot Microbiol* 1999;46:174–193.
26. Lynn DH. *The Ciliated Protozoa: Characterization, Classification and Guide to the Literature*, 3rd ed. Dordrecht: Springer; 2008. pp. 1–605.
27. Foissner W, Xu K. Monograph of the Spathidiida (Ciliophora, Haptoria). Vol. I: Protospathidiidae, Arcuospathidiidae, Apertospathulidae. *Monogr Biol* 2007;81:1–485.
28. Jankowski AW. Morphology and evolution of Ciliophora. III. Diagnoses and phylogenesis of 53 sapropelebionts, mainly of the order Heterotrichida. *Arch für Protistenkd* 1964;107:185–294.
29. Jankowski AW. Phylum Ciliophora Doflein, 1901. In: Alimov AF (editor). *Protista Part 2, Handbook on Zoology*. St. Petersburg: Russian Academy of Sciences, Zoological Institute; 2007. pp. 371–993.
30. Rotterová J, Bourland W, Čepička I. *Tropidoatractidae* fam. nov., a deep branching lineage of metopida (Armophorea, Ciliophora) found in diverse habitats and possessing prokaryotic symbionts. *Protist* 2018;169:362–405.

31. **Gutiérrez JC, Callejas S, Benïtez SBL, Martin-Gonzalez A, Martin-Gonzalez A *et al.*** Ciliate cryptobiosis: a microbial strategy against environmental starvation. *Int Microbiol* 2001;4:151–157.
32. **Gutiérrez JC, Diaz S, Ortega R, Martín-Gonzalez A.** Ciliate resting cyst walls: a comparative review. *Recent Res Dev Microbiol* 2003;7: 361–379.
33. **Kahl A.** Neu und ergänzende Beobachtungen heterotricher Ciliaten. *Arch für Protistenkd* 1927;57:121–203.
34. **Klein BM.** Das Silberliniensystem der Ciliaten. Weitere Ergebnisse. IV. *Arch Protistenkd* 1930;69:236–326.
35. **Kahl A.** Urtiere oder Protozoa I: Wimpertiere oder Ciliata (Infusoria) 3. Spirotricha. *Die Tierwelt Deutschlands* 1932;25:399–650.
36. **Dragesco J.** Les ciliés mésopsammiques littoraux: systématique, morphologie, écologie. *Des Trav la Stn Biol Roscoff* 1960:1–356.
37. **Alekperov IK.** New species of freshwater ciliates (Heterotrichida) from artificial water bodies of Azerbaijan. *Zool Zhurnal* 1984;63: 1731–1734.
38. **Foissner W.** Taxonomische studien über die Ciliaten des Grossglocknergebietes (Hohe Tauern, Österreich). IX. Ordnungen Heterotrichida und Hypotrichida. *Ber Nat-Med Ver Salzbg* 1980;5:71–117.
39. **Foissner W.** Colpodea (Ciliophora). *Protozoenfauna* 1993;4/1:1–798.
40. **Foissner W, Müller H, Agatha S.** A comparative fine structural and phylogenetic analysis of resting cysts in oligotrich and hypotrich Spirotrichea (Ciliophora). *Eur J Protistol* 2007;43:295–314.
41. **Takahashi E, Soichi I.** Light and scanning electron microscopy of Nyctotherus kyphodes (Ciliophora, Plagiotomidae) from the Galapagos giant tortoise, *Testudo* sp. *Bull Nippon Vet Zootech Coll* 1989; 38:9–15.